GEOPHYSICS, VOL. 75, NO. 6 (NOVEMBER-DECEMBER 2010); P. B221–B229, 10 FIGS.
10.1190/1.3505764

Case History

Using helicopter electromagnetic (HEM) surveys to identify potential hazards at coal-waste impoundments: Examples from West Virginia

Richard Hammack[1], Vlad Kaminski[2], William Harbert[3], Garret Veloski[1], and Brian Lipinski[4]

ABSTRACT

We have used 14 multifrequency helicopter-borne electromagnetic (HEM) surveys to determine the internal structure and integrity of mine-impoundment structures in West Virginia, U.S.A. — the first time such technology has been applied in this way and apparently well suited for such activities. The HEM surveys identified areas of concern in each of the impoundments investigated. In most cases, these were areas where filtrate was emerging high on the downstream embankment and represented an erosion risk. Of greater concern, the HEM survey identified thick bodies of slurry that remained unconsolidated and were buried deep beneath the embankment's crest of some impoundments. Ground confirmation activities indicated that HEM survey interpretations provided an accurate representation of the conductivity distribution within coal-waste impoundments. We then interpreted the conductivity/depth images from the HEM surveys to provide a snapshot of hydrologic conditions that existed within the impoundment at the time of the survey. Resistivity profiles were obtained at the inactive impoundment along segments of flight lines from the HEM survey. HEM and resistivity surveys detected a conductive layer at a depth of about 7 m that was interpreted to be unconsolidated coal slurry. The methods also detected conductive bodies at a depth of about 26 m that were interpreted to be flooded mine works. Resistivity surveys from these segments corroborated HEM data, thereby providing independent confirmation of the HEM data and its processing. The resistivity and HEM surveys indicated a resistive surface layer where the coarse coal refuse was placed. Beneath the resistive surface layer is a conductive layer of unconsolidated or partially consolidated coal slurry. These highly loaded bodies of unconsolidated slurry are susceptible to solifluction, which can threaten embankment stability. Underground mine workings were identified in the HEM data from one impoundment.

INTRODUCTION

Compromised coal-slurry impoundments represent a potential threat with respect to physical destruction and environmental pollution of surrounding regions. A coal-refuse impoundment consists of two major elements: the basin and the embankment. The basin is underlain by fine-grained coal waste that is delivered to the upstream side of the embankment via a slurry pipeline and released at a spigot point. (A more detailed description of the coal-waste impoundment structures with references is given in Appendix A.) Coal-slurry impoundment failure and solifluction, a type of mass wasting in which waterlogged sediments slowly move downslope, are concerns relevant to impounding structures.

Examples of impoundment failures include the Buffalo Creek and Inez failures (Davies et al., 1972). On 26 February 1972, a coal-waste impounding structure on Buffalo Creek in West Virginia, U.S.A., collapsed, releasing approximately 500 million liters (132 million gallons) of water (Davies et al., 1972). The resulting flood killed 125 people, injured 1100, and left more than 4000 homeless. Factors contributing to the impoundment failure included heavy

Manuscript received by the Editor 11 October 2009; revised manuscript received 3 March 2010; published online 20 December 2010.
[1]Department of Energy, National Energy Technology Laboratory, Pittsburgh, Pennsylvania, U.S.A. E-mail: richard.hammack@netl.doe.gov; garret.veloski@netl.doe.gov.
[2]University of British Columbia, Geophysical Inversion Facility, Vancouver, British Columbia, Canada. E-mail: kam3000@gmail.com.
[3]University of Pittsburgh, Department of Geology and Planetary Science, Pittsburgh, Pennsylvania, U.S.A. E-mail: harbert@pitt.edu.
[4]Atlas Energy Inc., Moon Township, Pennsylvania, U.S.A. E-mail: brian.lipinski@gmail.com.

rainfall and deficiencies in the foundation of the dam, which led to slumping and sliding of the waterlogged refuse bank. This disaster resulted in regulations that govern the design of embankment structures for new impoundments (National Research Council, 2002).

Since the implementation of regulations, no new embankments have failed. However, other types of impoundment failure have released water and coal slurry into streams. Some of these involved the breakthrough of water and coal slurry from impoundments into underground mines. The most notable incident occurred on 11 October 2000 near Inez, Kentucky, U.S.A., where 946 million liters (250 million gallons) of water and 117 million liters (31 million gallons) of coal slurry from an impoundment broke into an underground mine and flowed via mine workings into local streams (National Research Council, 2002). An estimated 1.6 million fish were destroyed along 120 km of stream, and temporary shutdowns were imposed on a large power plant and numerous municipal water supplies. As a result of the Inez incident, the U. S. Congress requested the National Research Council (NRC) to examine ways to reduce the potential for similar accidents in the future. The report, "Coal Waste Impoundments, Risks, Responses, and Alternatives" (National Research Council, 2002), documents the findings and recommendations of the NRC.

In response to the recommendations of the NRC, the Robert C. Byrd National Technology Transfer Center (NTTC) at Wheeling Jesuit University in Wheeling, West Virginia, U.S.A., contracted Fugro Airborne Surveys to conduct helicopter electromagnetic (HEM) surveys of 14 coal-waste impoundments in southern West Virginia (Figure 1). HEM geophysical imaging was used because it held the promise to determine or estimate structural integrity efficiently and to focus mitigation efforts accurately, if required, within the impoundment structures. The U. S. Department of Energy's National Energy Technology Laboratory (NETL) was asked to process, interpret, and validate survey data. Wheeling Jesuit University maintains a coal impoundment location and information system (http://www.coalimpoundment.org/) with additional details regarding all aspects of these structures in West Virginia.

Electromagnetic geophysical methods are well suited to investigate subsurface structure and hydrology of coal-slurry impoundments (Appendix A, Figure A-1). Coal-waste impoundments are predominantly constructed of coarse and fine coal waste, which can contain varying amounts of fluid. Coarse coal waste is used to construct the embankment of the impoundment because it is relatively homogeneous in physical properties and is therefore a predictable construction material (National Research Council, 2002). Slurry containing fine coal waste is hydraulically discharged into the decant pond where, as a result of engineered drainage, the material undergoes rearrangement because the coarsest material settles closer to the spigot point.

During refuse discharge, the processing fluid infiltrates through the coarse coal refuse in the embankment or invades adjacent aquifers. In typical impoundment construction, lifts of coarse coal refuse may be released over the unconsolidated material and may be further compacted with a bulldozer to decrease the pore space and therefore the amount of fluid in the material, at which point the amount of remaining fluid is of particular concern because of stability issues.

Construction and composition of these impoundments results in subsurface variation in sediments and hydrology related to leakage or subsidence. Most of these factors and other possible modes of failure can be identified by electromagnetic geophysical investigations and mitigated.

We believe this project is the first application of HEM for mapping impoundment structures and interpreting these results with respect to internal features. Earlier HEM research includes applications in mapping water quality (Sengpiel, 1983, 1986; Fitterman and Deszcz-Pan, 1998; Hammack and Mabie, 2002; Paine, 2003; Lipinski et al., 2008) and interpreting regional-scale lithologic variations (Christiansen and Christensen, 2003; B. D. Smith et al., 2003; R. S. Smith et al., 2004). Our methodology could be applied to almost all impoundment and coal-slurry impoundment structures to address questions relevant to their internal structural stability.

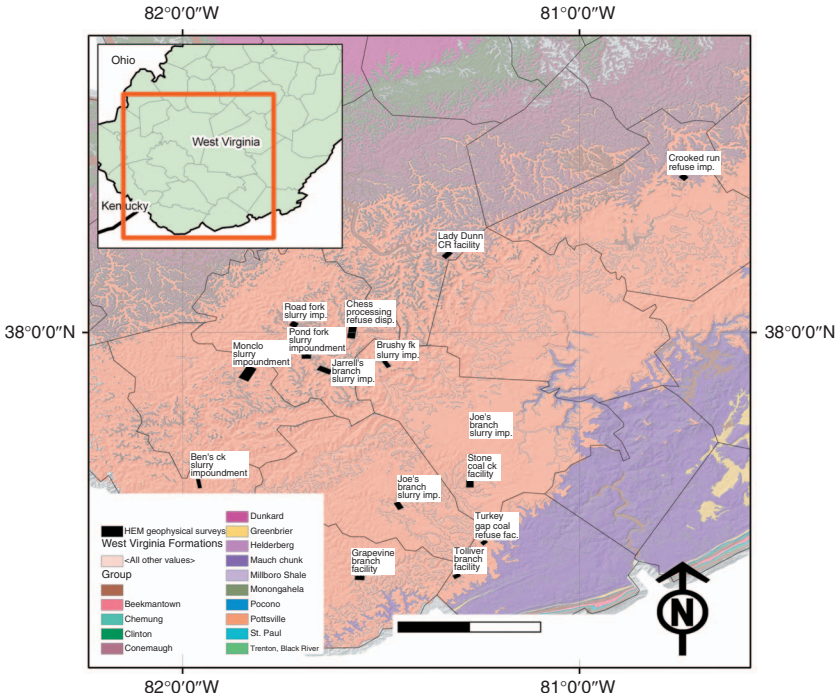

Figure 1. Location of 14 coal-waste impoundments surveyed using HEM. The inset shows the portion of West Virginia detailed in the larger map. Note the HEM survey locations, regional geology, and shaded relief included for reference. County boundaries of West Virginia are shown for spatial reference.

GEOPHYSICAL SURVEY DESCRIPTION

Site selection

Mine impoundments are ranked with respect to hazard potential based on the height of the embankment, the volume of material impounded, and the downstream effects of an impoundment failure (Mine Safety, 1974, 1983). Impoundments with moderate hazard potential are in predominately rural areas where failure may damage isolated homes or minor railroads, disrupting services or important facilities. Impoundments with a high hazard potential are those where failure could reasonably be expected to cause loss of hu-

man life and serious damage to houses, industrial and commercial buildings, important utilities, highways, and railroads.

The NTTC selected 14 impoundments for HEM geophysical surveys in southern West Virginia; these sites were given a moderate or high hazard-potential rating. This list of selected impoundments was transferred to the NETL, where flight areas were determined by constructing a bounding rectangle that enclosed the impoundments and ancillary structures, including a 1-km-wide buffer around the impoundments to determine the flight area. An effort was made to include sites with known underground mines in the surveyed areas. The locations for surveyed impoundments are depicted in Figure 1.

Data acquisition

In July 2003, Fugro Airborne Surveys performed frequency-domain electromagnetic (FDEM) surveys of the selected coal-refuse impoundments using the RESOLVE electromagnetic data acquisition system. This system consists of five coplanar transmitter/receiver coil pairs operating at frequencies of approximately 385 Hz, 1.70 kHz, 6.20 kHz, 28.1 kHz, and 116 kHz and one coaxial transmitter/receiver coil pair that operates at 1.41 kHz. Separation for the five coplanar coil pairs was 7.9 m; separation for the coaxial coils was 9 m. (A complete description of the RESOLVE data acquisition system is available at http://www.fugroairborne.com.) An optically pumped cesium vapor magnetometer mounted within the RESOLVE sensor was used to acquire total-field magnetic data concurrent with the collection of electromagnetic data.

The surveys were flown using an Ecureuil AS350-B2 helicopter, with the RESOLVE sensor suspended about 30 m beneath the helicopter. A radar sensor-measured instrument altitude, which averaged 45 m because of the rugged terrain, trees, and numerous power lines. The acquisition geometry consisted of parallel flight lines separated by approximately 50 m. At the average flight speed of 90 km/hour, the 10-Hz data-acquisition rate resulted in one HEM sounding every 2.5 m along the flight line.

Data processing

Preliminary data processing, including leveling and digital filtering, was performed by Fugro, which base-leveled the data to remove temperature-related drift and low-frequency noise spikes using a spherical rejection median filter (Cain, 2003) and high-frequency noise using a low-pass spatial-domain filter with Hanning coefficients at the roll-off (Cain, 2003). In-phase and quadrature data were leveled to remove differences related to variation in instrument calibrations. Electronic data were then transmitted to NETL for additional processing, analysis, and interpretation. These data included apparent-conductivity maps calculated using the Fraser (Fraser, 1978) algorithm for six frequencies, total magnetic field intensity map, leveled in-phase and quadrature data, and navigational data. Space limitations preclude a detailed description of these processing steps for our survey. Leveling and calibration relevant to FDEM systems are presented in Brodie et al. (2004) and Brodie and Sambridge (2006).

The HEM data were then processed to calculate the subsurface conductivity distribution with respect to depth along each flight line. This can be done using two classes of methods: (1) conductivity depth transforms (CDTs) or (2) layered-earth inversions (LEIs) (Sattel, 2005). For our research, we used two CDT algorithms — the centroid depth algorithm as implemented in EMIGMA (Sengpiel, 1988; Sengpiel and Siemon, 2000) and the method of Macnae et al. (1998) as implemented in EMFLOW (Macnae et al., 1991) — to preprocess the data and guide parameter selection for a more rigorous LEI model, EM1DFM.

EM1DFM fits a modeled response to the input data by minimizing an objection function and provides error responses between the input data and model output so that the model can be evaluated (University of British Columbia, 2000; Farquharson et al., 2003). Data were inverted to an earth model composed of 80 horizontal layers, each 1 m thick, with a starting-conductivity model and reference-

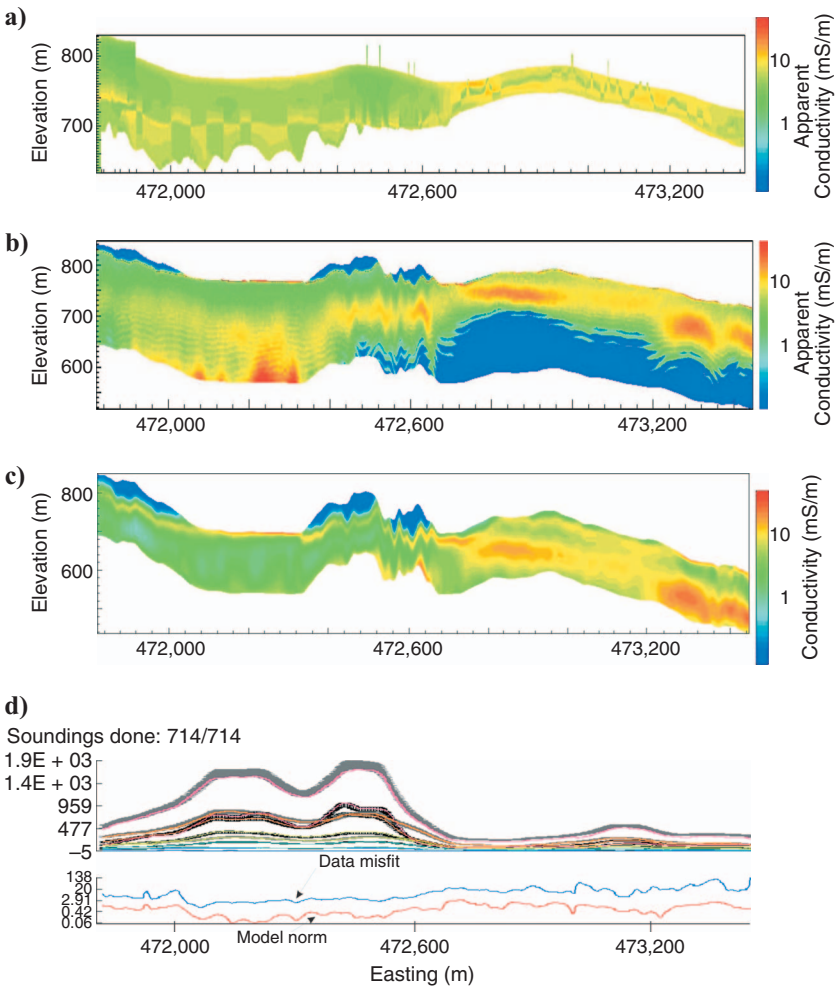

Figure 2. Comparison of methods used to determine subsurface apparent conductivity or conductivity (EM1DFM does a full inversion for conductivity) using a representative HEM CDI profile 130110: (a) EMIGMA, (b) EMFLOW, and (c) EM1DFM. (d) Data profile for the frequencies used to determine apparent conductivity and the associated data misfit and model norm.

conductivity model of 10 mS/m. After comparing results from EMIGMA and EMFLOW with EM1DFM results (Figure 2), we completed inversions using the fixed trade-off parameter β algorithm within EM1DFM for $\beta = 10$ after trial inversions indicated this was the optimal value. Data-error values were determined to be approximately 5%, consistent with previous research (Tølbøll and Christensen, 2006). The values of the smallest and flattest components of the model structure term were 0.001 and 1, respectively.

Conductivity depth sections were related to features on maps and air photos using software developed at NETL. Within the Geographical Information Systems (GIS) environment, the locations of conductivity anomalies could be related to specific attributes of the coal-refuse impoundment as well as the locations of known underground mine workings. Another assumption was that among dry, coarse refuse, high-clay-mineral content can increase electrical conductivity as well. The conductivity models have values of 0–200 mS/m and are indicated with a color ramp of blue (resistive) to red (conductive) in Figure 2. To validate our HEM data, ground geophysical surveys were completed at selected locations.

Ground surveys

Revistivity ground surveys were conducted at three impoundments to validate the HEM results. These surveys used the Supersting R8 IP and Supersting + 28 R8 IP instruments with 56-electrode Swift cables and 28-electrode passive cables, respectively. Electrode spacing was 1–6 m, depending on the spatial area surveyed; most commonly, electrode spacing was 4 m. Resisivity profiles were obtained along selected segments of flight lines or across push-outs using a single cable deployment. The 28-electrode passive cables were used for flight line segments, and 56-electrode Swift cables were used for push-outs. Electrodes were polled with a dipole-dipole array, and resulting data were processed using Advanced Geosciences Inc. resistivity imaging software (http://www.agiusa.com/datasheets/AGIEarthImager.pdf). Inverted resistivity data were further converted to conductivity and displayed as conductivity-depth profiles.

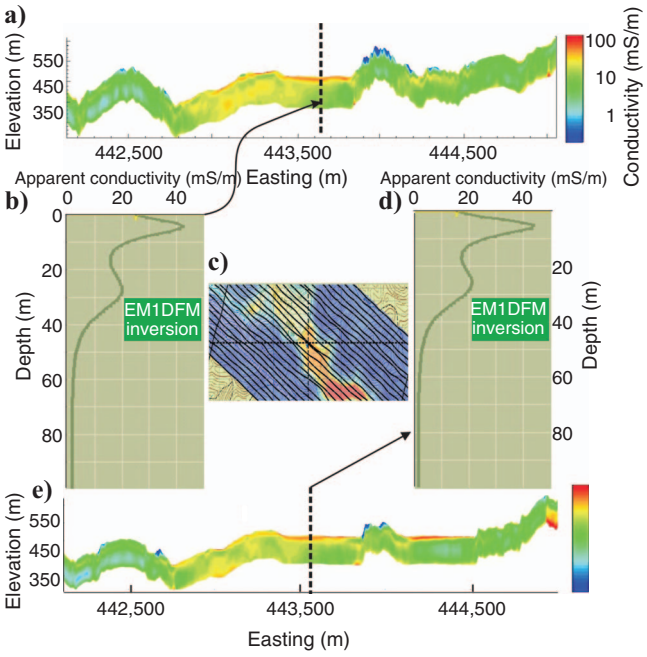

Figure 3. The reproducibility of HEM data. Two adjacent flight lines overlap briefly, resulting in coincident data points. (a) CDI for profile 70,140, (e) CDI for 70,150, (c) flight lines and conductivity calculated from the highest frequency. (b, d) EM1DFM-calculated conductivity/depth profiles generated from HEM data are similar at coincident points, although flight directions were opposite. The dashed vertical line shown in the center of (a) shows the location of the profile in (b); the dashed vertical line shown in the center of (e) shows the location of the profile in (d). We interpret the change in conductivity with depth to denote the boundary between the unsaturated zone (resistive) and saturated zone or water table (conductive). The upper 100 m of the CDI is used for interpretation; conductors below this depth are assumed to be artifacts of the processing or noise.

RESULTS AND DISCUSSION

HEM data reproducibility

In this study, we found HEM geophysical data to be highly reproducible based on careful review of coincident flight lines and tie points within individual surveys. Figure 3 demonstrates the reproducibility of the calculated conductivity results in a region where flight lines overlap because sudden wind gusts displaced the helicopter temporarily from the survey flight-line course but allow direct comparison of repeat HEM measurements over the same spatial location. In the location shown in Figure 3d, measurements on adjacent lines were within a few meters, well within the footprint of the HEM sensor, which is essentially a circular area with a 30-m radius centered on ground directly below the sensor. The conductivity/depth images (CDIs) for the two flight lines are similar, and conductivity/depth profiles (sounding profiles below CDIs) are nearly identical at the coincident location. This provides assurance that the HEM sensor is responding to conditions specific to that location and that the results are reproducible. With some HEM systems, there is directional offset in the data collection so that the data are dependent on flight direction. Because results were identical at such coincident locations, in this case, even though flight directions were 180° apart, we are confident of the reproducibility of these HEM surveys.

Ground verification of HEM data

Geophysical data ground verification at three impoundments (Brushy Fork, Jarrell's Branch, and Monclo) was completed during the summer and fall of 2005, two years after the HEM surveys were flown. The Brushy Fork and Monclo impoundments are large upstream structures, whereas the Jarrell's Branch impoundment is a downstream structure. Interviews with company staff engineers responsible for constructing the impoundments provided additional information to facilitate the interpretation of geophysical data. In general, the engineers found the preliminary HEM interpretations to be accurate based on their knowledge of site hydrology and confirmed the accuracy of mapping the engineered drains and potentially flooded subsurface voids.

Our main challenge in comparing the HEM geophysical surveys with our ground surveys was that the helicopter surveys were flown in 2003 and the ground geophysics occurred two years later. Two out of three impoundments selected for ground geophysical surveys were active and had been modified significantly because large quantities of coal waste were being disposed there continually. According to the project engineers, about 350,000 tons of coarse coal waste was being placed on the embankment at the Brushy Fork impoundment each month. Therefore, the structural and hydrologic condi-

tions that existed during the 2003 HEM survey might have changed significantly by 2005, when ground resistivity surveys took place. For this reason, our primary focus in the activity to use ground-based geophysical resistivity surveys to verify and compare with the HEM surveys occurred at the Monclo impoundment, which was inactive between the time of the helicopter and ground surveys (Figures 3 and 4).

An HEM conductivity-depth section for a segment of flight line 60270 is compared to a resistivity profile (plotted as conductivity) acquired on the ground at the same location in Figure 4. Two segments of adjacent flight lines (60,270 and 60,280) that crossed the decant pond (now dry) within the Monclo impoundment were chosen for a resistivity ground survey. Both geophysical apparent-conductivity cross sections (Figure 4a and c) show a low-conductivity (5–20-mS/m) surface layer 2–5 m thick, which is predominantly coarse coal waste. Beneath the resistive surface layer is a conductive layer that is discontinuous in the resistivity data but continuous in the HEM data. This is because the spatial resolution of the HEM instrument provides less discrete imaging capabilities than the 4-m spaced electrode array configuration used in the ground geophysical resistivity survey at this site. However, the interpreted depths to this conductive layer derived from the data sets agree well with each other, suggesting that both geophysical survey methods allow imaging of the same overall apparent conductivity subsurface structure. Beneath this conductive layer, at the bottom of the cross section, is a thick resistive layer that contains two conductive anomalies visible in the HEM data (at about 25 and 40 m of depth, respectively). Only the uppermost is within the exploration limits of the conducted dipole-dipole ground resistivity survey. We interpret this feature to be flooded mine working.

Other ground-survey-based resistivity data were obtained from an active push-out at the Jarrell's Branch impounding structure (Figure 5). The HEM results from the 2003 survey were compared with ground-survey resistivity results from 2005, despite the fact that the 2005 impoundment structure push-outs were in a different location. Nonetheless, the resistivity profiles showed reasonable similarity with the HEM conductivity results. Both data sets show a resistive surface layer that we know to be coarse coal waste, emplaced on the surface of the push-out. The resistive layer is thicker in the 2005 resistivity by roughly 12 m. Beneath the resistive overburden is a conductive layer, which we interpret to be unconsolidated coal refuse. The recovered conductivity and thickness of this layer is remarkably similar in the 2005 resistivity profile and in a spatially coincident 2003 HEM conductivity sounding (Figure 5d).

Finally, at the base of the cross section is a resistive bedrock layer that defines the bottom of the decant pond. The distribution of conductivity beneath this push-out supports our assumption that the calculated conductivity displayed in the conductivity model is proportional to the material's water content. This conclusion, therefore, suggests that our HEM results can be used to map unconsolidated slurry, which could represent a significant embankment stability hazard. Based on these HEM and ground geophysical survey comparisons, it is conclusive that recovered depths and modeled conductivities from airborne surveys are accurate and can be acquired at significantly lower cost per line-km than ground-based geophysics surveys.

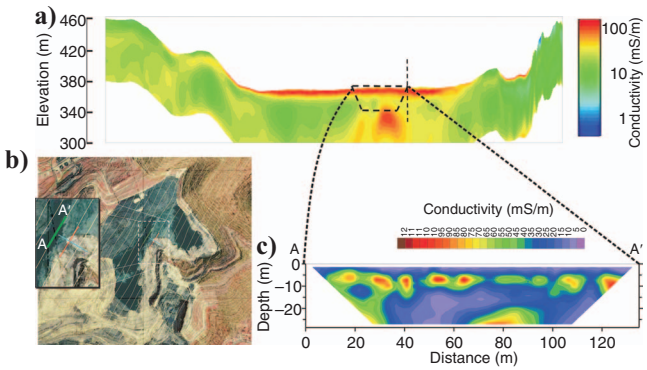

Figure 4. (a) CDI for line 60270 calculated from the HEM survey compared with (c) a ground-based resistivity survey for a segment of a flight line crossing the Monclo impoundment, shown as (b) a digital orthophoto. In (b), note the locations of flight lines from the helicopter survey (light yellow). Inset map shows the location of three resistivity profiles acquired to corroborate helicopter survey results. Different color values are used for (a) and (c).

ELECTROMAGNETIC MAPPING OF COAL-WASTE IMPOUNDMENTS

The HEM response to different materials within the coal-waste impoundment depends largely on the porosity of the material and the degree of water saturation. This is because the electrical conductivity of impoundment TDS-rich fluid is much greater than the bulk conductivity of dry coal refuse. Coal-slurry water exhibits lower pH and increased mineral content, total dissolved solids, electrical conduc-

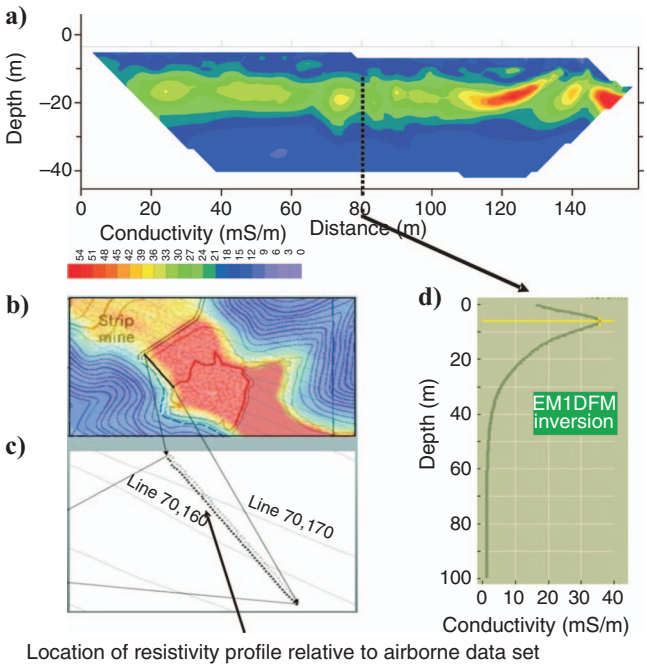

Figure 5. Comparison between (a) ground-based resistivity data (upper-conductivity depth profile) and (d) conductivity calculated by EM1DFM using HEM data (lower-conductivity/depth section or sounding) acquired over a push-out at the Jarrell's Branch impoundment. The dashed vertical line shows approximately where the where HEM flight line intersected the resistivity profile. The resistive surface layer is thicker in the resistivity profile because more coarse coal waste was placed here between the HEM survey and the resistivity survey. (b) Map view of conductivity calculated by EM2DFM using HEM data. (c) Location of two specific flight lines.

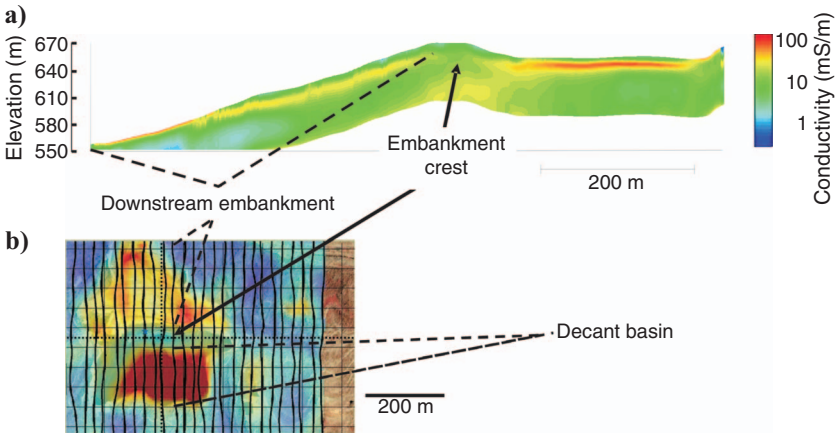

Figure 6. (a) CDI for line 100,180 of East Gulf, calculated from HEM data collected over a coal-waste impoundment and showing regions of high conductivity (red and yellow), which are interpreted to be areas of greater water content. (b) Conductivity map for the highest frequency collected, clearly showing the geometry of the impoundment.

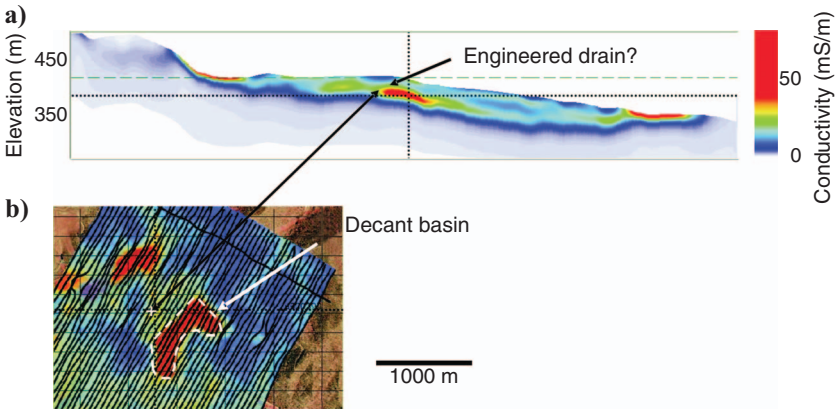

Figure 7. (a) CDI calculated from HEM data, showing the location of a strong conductor in the downstream embankment of an impoundment. The conductor was originally thought to be a finger drain but was later found to be the location of a buried concrete spillway. (b) Conductivity map for the highest frequency collected, showing the geometry of the impoundment.

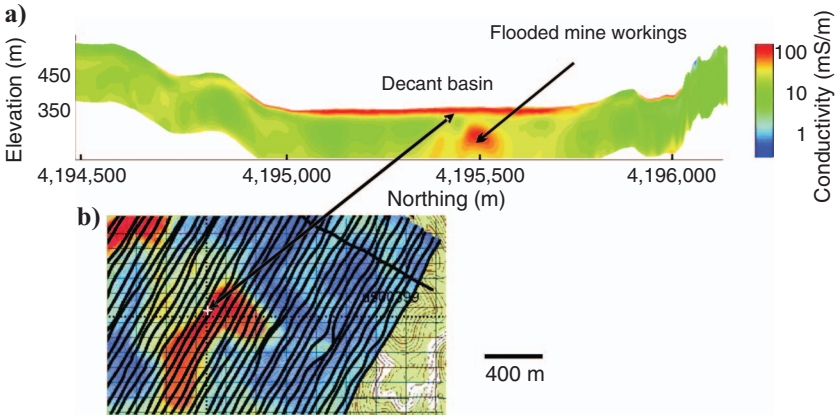

Figure 8. (a) CDI for line 60,270, Monclo impoundment, calculated from HEM data and showing a discontinuous deep conductor that may represent flooded mine works. (b) Conductivity map for the highest frequency collected, showing the geometry of the impoundment.

tivity, and sulfates (Olem, 1981; Olem and Betson, 1985). Saturated material with high porosity is the most conductive. Saturated, well-compacted material (lower porosity) is therefore less conductive. The least conductive material is poorly compacted, air-filled coarse coal waste, which is placed above the water table. Hence, HEM data can provide a clear demarcation between the vadose and phreatic zones within the embankment as a result of significant conductivity differences between saturated and unsaturated material. When material is obviously below the water table, HEM data can indicate porosity because material with greater effective pore space will be more electrically conductive.

In Figure 6, the HEM-derived conductivity model shows a cross section for flight line 100180, which crosses a normally seeping impounding structure. Figure 6b shows a georeferenced orthophoto with a 25-KHz conductivity grid and superimposed HEM survey flight path. The decant basin is the most conductive part of a coal-waste impoundment because it often contains conductive, standing TDS-rich water up to several meters in thickness. The embankment crest is usually the least conductive area because it is composed of uncompacted coarse coal waste and is located above the water table. The downstream embankment commonly contains subsurface conductive layers that represent the groundwater seepage paths underneath the embankment, which are usually engineered to emerge at the base of the dam (toe drains).

The HEM-derived conductivity depth section shown in Figure 7 was produced from flight line 60,210, which is downstream from and subparallel to the crest of an impoundment embankment. A deep conductor is present in the conductivity model and is interpreted as an engineered drain — essentially a buried concrete spillway. This interpretation was validated following our analysis by project engineer John McDaniels, who confirmed this subsurface structure was present and had been designed to route pond waters to prevent overtopping.

Figure 8 is an HEM-derived conductivity depth section from flight line 60,270, which crosses the decant basin of the Monclo impoundment. This figure depicts conductive targets interpreted as flooded abandoned mine workings. The interpreted flooded mine workings correspond depthwise to the location of the commercial Winnifrede Coal, which supposedly was mined from a strip bench and is now buried beneath the decant pond. The escape of unconsolidated waste as a result of subsidence is another known mechanism of impoundment failure and therefore required thorough attention. Such scenarios can be difficult using drilling; however, an HEM survey can quickly detect pockets of unconsolidated refuse.

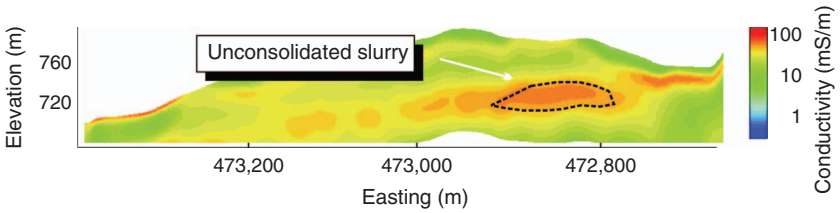

Figure 9. CDI for line 130,110, McComas impoundment, calculated from HEM data and showing a pocket of unconsolidated slurry buried 38 m deep in the embankment.

Figure 9 shows another HEM-derived conductivity depth section from flight line 130,110, which is interpreted to reveal a pocket of unconsolidated material approximately 35–40 m below the top of the embankment of the McComas impoundment. Such plumes may cause structural instability by solifluction, the movement of water-saturated soil material, in the impoundment feature. The accurate imaging of such subsurface features is an important result of our geophysical study and could be widely useful with respect to mitigating hazards related to impoundment structures. For example, HEM geophysical imaging could help efficiently determine structural integrity and focus mitigation efforts accurately within the impoundment structures.

CONCLUSIONS

HEM surveys provide a 3D picture of the conductivity distribution within coal-waste impounding structures. NETL personnel have used ground resistivity surveys to confirm the accuracy of HEM results. For our study, TDS-rich water was assumed to be the most conductive component of the material. Hydrologic interpretations using HEM data appear to justify this assumption. However, if hydrologic interpretations based on HEM data are to be used for regulatory decisions, the interpretations must be substantiated with results from monitoring groundwater wells. We suggest that HEM results be used to define the spatial locations for follow-up ground-based investigations that can measure physical or hydrologic properties directly.

Our study suggests that conductivity-depth models generated from HEM data can be used to map hydrologic and subsurface structural features of the study's impoundment sites. For example, the subsurface pathways taken by filtrate through the embankment can be discerned easily by following conductors from the decant pond through the embankment until they emerge on the downstream face. It is possible to predict areas prone to springs and seeps by noting where conductors are at or near the surface. In addition, HEM is able to detect flooded mine workings adjacent to the impounding structures as well as identify pockets of unconsolidated slurry in the decant pond or beneath the embankment.

Hydrologic features detectable by HEM have been linked to past impoundment failures. For example, HEM should be able to depict the location of the phreatic surface between the decant basin and its emergence on the downstream slope of the embankment. This knowledge will help identify sites of internal erosion (piping) or surface erosion.

Airborne geophysical mapping technology as applied to impounding structure safety analysis is therefore robust and strongly suggested for future studies of similar sites. It is a significant conclusion of this study that HEM technology adds subsurface structural quality assurance; utilizing these geophysical data, potential hazards can be identified and mitigated.

ACKNOWLEDGMENTS

The authors acknowledge the National Technology Transfer Center for contracting HEM surveys of the 14 coal-refuse impoundments in southern West Virginia and for providing funding to NETL to process, interpret, and validate data resulting from these surveys. This work could not have been completed without the University of British Columbia's Geophysical Inversion Facility EM1DFM inversion code, which was provided to the University of Pittsburgh. We deeply appreciate their generosity and their philosophy in science and research. We thank Hansruedi Maurer and the reviewers of this article for suggesting modifications that considerably improved our final manuscript. The help of Sheral Danker of SEG and of Kathryne Pile is also gratefully acknowledged.

APPENDIX A

REVIEW OF IMPOUNDMENT STRUCTURES

A coal-refuse impoundment consists of two major elements: the basin and the embankment (Figure A-1). The basin is underlain by fine-grained coal waste, which is delivered to the upstream side of the embankment via a slurry pipeline and released at a spigot point. The spigot point is moved periodically across the embankment face, thereby creating a series of coalescing, deltaic depositional structures where coarser material accumulates in the vicinity of the spigot point and finer material is carried farther away. The flooded portion of the basin is sometimes called a decant pond because clarified water is returned to the coal-cleaning plant for reuse when sedimentary particles have settled out of the slurry. The basin is bounded on the upstream side by valley walls and on the downstream side by the embankment, which is a damlike structure that consists of coarse-grained coal waste sometimes mixed with clay or gravel to alter its permeability. While the impoundment is active, the embankment is constantly being raised to provide more space for coal-waste disposal.

Impoundment structures may incorporate three types of embankment-raising operations: (1) upstream, the most common type for coal-waste impoundments; (2) centerline, used for true dams; and (3) downstream, the most stable structure, used at sites with high ratios of coarse-to-fine coal waste (Figure A-1). An upstream embankment is raised by placing lifts of coarse material on the top of the embankment and on the fine refuse in the basin near the embankment. The area of the basin where coarse coal waste is mechanically placed over unconsolidated fine coal waste is termed a *push-out*.

Two important factors relevant to embankment stability are control of internal erosion, referred to as *piping*, and erosion of the downstream face of the embankment. These can be controlled by engineering the embankment structure so that the hydraulic conductivity increases in a downstream direction, thereby ensuring that any seepage will emerge low on the downstream face of the embankment. In addition, many embankments contain surface and subsurface drains to intercept seepage and safely convey it away from the embankment face. The embankment is designed to isolate the coal-

slurry refuse, prevent migration of fine sediments, and minimize water pressure and piping on the downstream side of the embankment (National Research Council, 2002).

Piping is a subsurface erosion process that can occur when there are fluid-flow pathways large enough for soil particles to be transported with the seeping liquid. Piping can be reduced by installing filter and drain zones within the embankment that collect and route water to the downstream toe of the embankment (National Research Council, 2002). In addition to the toe drain, several other drain types, including chimney drains, finger drains, and blanket drains, can be incorporated into impoundment structures to reduce or eliminate piping. Monitoring filtrate propagation through the coarse coal refuse and engineered drains is an important aspect in evaluating safety of an impoundment.

Failure models of a coal-slurry impoundment include embankment and basin. An embankment or basin can fail in several ways. A primary factor is the type of embankment construction. Slope instability and earthquake effects dominate failures of upstream embankments, but foundation failure is more likely to occur in downstream embankments. Overtopping is another cause of impoundment failure; it results when inflow exceeds the storage capacity of the impoundment. Basin failure is most likely to occur in areas where current or past mining is near the impoundment. Unfortunately, the location of underground mines is often inaccurate because subsurface mine maps are often uavailable (Ramani et al., 2002).

Factors that must be considered to prevent basin failure are subsidence, excessive seepage, and internal erosion. In response to the immediate roof caving into the workings and floor subsidence, subsidence disturbs the strata above and adjoining the mining area (National Research Council, 2002) and results in opening tensile cracks on the surface, displacement along faults and joints, and some distortion of the strata around the working.

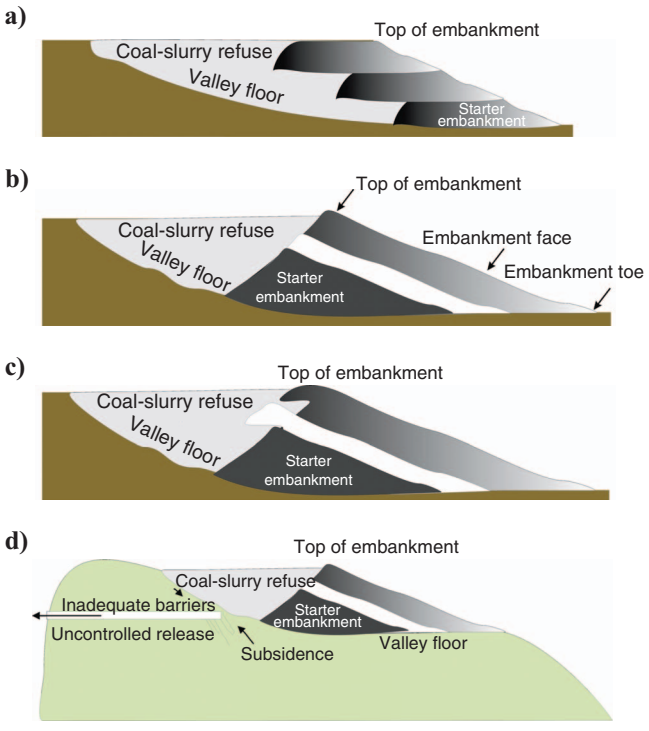

Figure A-1. Impoundment types: (a) upstream, (b) downstream, and (c) centerline. (d) Possible failure mechanisms related to subsidence and abandoned underground mine workings beneath the coal-slurry refuse. Details regarding the physical, chemical, and electrical conductivity characteristics of coal slurry can be found in Olem (1981) and Olem and Betson (1985).

REFERENCES

Brodie, R. C., A. A. Green, and T. J. Munday, 2004, Calibration of RESOLVE airborne electromagnetic data — Riverland and East Tintinara, South Australia: Cooperative Research Centre for Landscapes, Environment and Mineral Exploration Open File Report 173, http://crcleme.org.au/Pubs/OPEN%20FILE%20REPORTS/OFR%20171-180/OFR173.pdf, accessed 1 March 1 2010.

Brodie, R., and M. Sambridge, 2006, A holistic approach to inversion of frequency-domain airborne EM data: Geophysics, **71**, no. 6, G301–G312, doi: 10.1190/1.2356112.

Cain, M. J., 2003, Helicopter-borne RESOLVE EM and magnetic geophysical survey, Charleston to Bluefield, West Virginia: Fugro Airborne report for the U. S. Department of Energy.

Christiansen, A. V., and N. B. Christensen, 2003, A quantitative appraisal of airborne and ground-based transient electromagnetic (TEM) measurements in Denmark: Geophysics, **68**, 523–534, doi: 10.1190/1.1567221.

Davies, W. E., J. F. Bailey, and D. B. Kelly, 1972, West Virginia's Buffalo Creek flood: A study of the hydrology and the engineering geology: U. S. Geological Survey Circular 667.

Farquharson, C. G., D. W. Oldenburg, and P. S. Routh, 2003, Simultaneous 1D inversion of loop-loop electromagnetic data for both magnetic susceptibility and electrical conductivity: Geophysics, **68**, 1857–1869, doi: 10.1190/1.1635038.

Fitterman, D. V., and M. Deszcz-Pan, 1998, Helicopter EM mapping of saltwater intrusion in Everglades National Park, Florida: Exploration Geophysics, **29**, no. 2, 240–243, doi: 10.1071/EG998240.

Fraser, D. C., 1978, Resistivity mapping with an airborne multicoil electromagnetic system: Geophysics, **43**, 144–172, doi: 10.1190/1.1440817.

Hammack, R. W., and J. S. Mabie, 2002, Airborne EM and magnetic surveys find fault(s) with Sulphur Bank mercury mine Superfund site: The Leading Edge, **21**, 1092–1095, doi: 10.1190/1.1523750.

Lipinski, B. A., J. I. Sams, B. D. Smith, and W. Harbert, 2008, Using HEM surveys to evaluate disposal of by-product water from CBNG development in the Powder River basin, Wyoming: Geophysics, **73**, no. 3, B77–B84, doi: 10.1190/1.2901200.

Macnae, J., A. King, N. Stolz, A. Osmakoff, and A. Blaha, 1998, Fast AEM processing and inversion: Exploration Geophysics, **29**, no. 2, 163–169, doi: 10.1071/EG998163.

Macnae, J. C., R. Smith, B. D. Polzer, Y. Lamontagne, and P. S. Klinkert, 1991, Conductivity-depth imaging of airborne electromagnetic step-response data: Geophysics, **56**, 102–114, doi: 10.1190/1.1442945.

Mine Safety Health Administration, 1974, Design guidelines for coal refuse piles and water, sediment, or slurry impoundments, and impounding structures: U. S. Department of Labor Informational Report 1109.

———, 1983, Design guidelines for coal refuse piles and water, sediment, or slurry impoundments, and impounding structures: Amendment to U. S. Department of Labor Informational Report 1109.

National Research Council, 2002, Coal waste impoundments: Risks, responses and alternatives: National Academy Press.

Olem, H., 1981, Coal and coal mine drainage: Journal Water Pollution Control Federation, **53**, 814–824.

Olem, H., and R. P. Betson, 1985, Coal and coal mine drainage: Journal Water Pollution Control Federation, **57**, 591–596.

Paine, J., 2003, Determining salinization extent, identifying salinity sources, and estimating chloride mass using surface, borehole, and airborne electromagnetic induction methods: Water Resources Research, **39**, no. 3, 1059–1069.

Ramani, R., H. William, F. Kirby, J. Kohler, S. Kravits, J. Lamont, J. Robers, D. Smith, and J. Szalankiewicz, 2002, Report of the Governor's Commission on Abandoned Mine Voids and Mine Safety: State of Pennsylvania Department of Environmental Protection, http://www.dep.tate.pa.us/hosting/mnesafetycommission, accessed September 2010.

Sattel, D., 2005, Inverting airborne electromagnetic (AEM) data with Zohdy's method: Geophysics, **70**, no. 4, G77–G85, doi: 10.1190/1.1990217.

Sengpiel, K. P., 1983, Resistivity/depth mapping with airborne electromagnetic survey data: Geophysics, **48**, 181–196, doi: 10.1190/1.1441457.

———, 1986, Groundwater prospecting by multifrequency airborne electromagnetic techniques: Geological Survey of Canada Special Paper 86–22, 131–138.

———, 1988, Approximate inversion of airborne EM data from a multilayered ground: Geophysical Prospecting, **36**, no. 4, 446–459, doi: 10.1111/j.1365-2478.1988.tb02173.x.

Sengpiel, K. P., and B. Siemon, 2000, Advanced inversion methods for AEM

exploration: Geophysics, **36**, 446–459.
Smith, B. D., D. V. Smith, P. L. Hill, and V. F. Labson, 2003, Helicopter electromagnetic and magnetic survey data and maps, Seco Creek area, Medina and Uvalde Counties, Texas: U. S. Geological Survey Open-File Report 03-0226.
Smith, R. S., M. D. O'Connell, and L. H. Poulsen, 2004, Using airborne electromagnetic surveys to investigate the hydrogeology of an area near Nyborg, Denmark: Near Surface Geophysics, **3**, 123–130.
R. J. Tølbøll, and N. B. Christensen, 2006, Robust 1D inversion and analysis of helicopter electromagnetic (HEM) data: Geophysics, **71**, no. 2, G53–G62, doi: 10.1190/1.2187752.
University of British Columbia, 2000, EM1DFM: A program library for forward modeling and inversion of frequency domain electromagnetic data over 1D structures, version 1.0: University of British Columbia Geophysical Inversion Facility.